VOLUME 111, NUMBER 16
AUGUST 2, 1989

JOURNAL
OF THE
AMERICAN
CHEMICAL
SOCIETY

Kinetics and Mechanism of Halogen-Atom-Transfer Reactions between Haloalkanes and Several 17-Electron Transition-Metal Complex Negative Ions in the Gas Phase[1]

Michael T. Jones, Richard N. McDonald,* Philip L. Schell, and Mohammed H. Ali

Contribution from the Department of Chemistry, Kansas State University, Manhattan, Kansas 66506. *Received December 7, 1988*

Abstract: The rate constants for the halogen-atom-transfer reactions between 11 17-electron transition-metal complex anion radicals ($L(OC)_{x-1}M^{\bullet -}$) and up to 14 halogenated methanes and ethanes (RX) were measured in a flowing afterglow apparatus at 298 K. Failure to correlate the kinetic data vs $D°(R-X)$ ruled out simple halogen-atom abstraction as the mechanism for these reactions. While the thermodynamic EA(RX) failed to correlate the rate constants, correlations of these kinetic data were achieved vs the rate constants (k_{TEA}) and activation energies (E^*) for thermal electron attachment to the haloalkanes. On the basis of these correlations and the absence of X^- or $RX^{\bullet -}$ as products in these reactions, the mechanism of these halogen-atom transfers is assigned to be electron transfer in the initially formed ion/neutral collision complex $[L(OC)_{x-1}M^{\bullet -}/RX]$ yielding $[L(OC)_{x-1}M/RX^{\bullet -}]$ followed by X^- transfer ($RX^{\bullet -}$ dissociation) giving $[L(OC)_{x-1}MX^-/{}^\bullet R]$ and separation producing the observed product $L(OC)_{x-1}MX^-$. The results allow lower limits to be placed on a series of metal–halogen bond energies, $D°(L(OC)_{x-1}M^--X)$, in the product negative ion complexes.

The transfer of a halogen atom from alkyl halides to transition-metal-centered free-radical complexes is an interesting subset of oxidative addition reactions with a one-electron change occurring at the metal.[2] Two mechanisms have been considered for the generation of the product metal halide complexes L_nM-X: (i) atom abstraction (eq 1) ligand in the coordination sphere of

$$L_nM^\bullet + XR \rightarrow [\underset{\mathbf{1}}{L_nM\text{–}X\text{–}R}] \rightarrow L_nMX + {}^\bullet R \qquad (1)$$

M with structure **1** as an intermediate or transition state; (ii) electron transfer followed by transfer of X^- from $RX^{\bullet -}$ to L_nM^+ in **2** (eq 2). The atom abstraction mechanism in eq 1 is typical

$$L_nM^\bullet + RX \rightarrow [\underset{\mathbf{2}}{L_nM^+RX^{\bullet -}}] \rightarrow L_nMX + {}^\bullet R \qquad (2)$$

of an inner-shere process, while the electron-transfer mechanism in eq 2 would be characterized as an outer-sphere process. In the condensed phase, 17-electron transition-metal carbonyl radicals are generated by several means, including flash photolysis and pulse radiolysis of various metal carbonyl dimers.[3] Several groups have reported that the halogen-atom transfer reactions to the 17-electron metal complexes $CpW(CO)_3$,[4,5] $Mn(CO)_5$,[5,6] and $Re(CO)_5$[5] from haloalkanes occurred by halogen-atom abstraction (eq 1). However, Brown et al.[7,8] recently reported that electron transfer (eq 2) is a significant component in the halogen-atom

(1) Presented in part at the 191st ACS Meeting, New York, NY, 1986; Phys 112.
(2) (a) Collman, J. P.; Hegedus, L. S.; Norton, J. R.; Finke, R. G. *Principles and Applications of Organotransition Metal Chemistry*; University Science Books: Mill Valley, CA, 1987; Chapter 5. (b) Kochi, J. *Organometallic Mechanisms and Catalysis*; Academic Press: New York, 1978; Chapter 7.
(3) Reviews on this subject include: (a) Kochi, J. K. *J. Organomet. Chem.* **1986**, *300*, 139. (b) Meyer, T. J.; Caspar, J. V. *Chem. Rev.* **1985**, *85*, 187. (c) Geoffrey, G. L.; Wrighton, M. S. *Organometallic Photochemistry*; Academic Press: New York, 1979; (d) Lappert, M. F.; Lednor, P. W. In *Advances in Organometallic Chemistry*; Stone, F. G. A., West, R., Eds.; Academic Press: New York, 1976.
(4) Laine, R. M.; Ford, P. C. *Inorg. Chem.* **1977**, *16*, 388.
(5) Hepp, A. F.; Wrighton, M. S. *J. Am. Chem. Soc.* **1981**, *103*, 1258.
(6) Herrick, R. S.; Herrinton, T. R.; Walker, H. W.; Brown, T. L. *Organometallics* **1985**, *4*, 42.
(7) Lee, K.-W.; Brown, T. L. *J. Am. Chem. Soc.* **1987**, *109*, 3269.
(8) Hanckel, J. M.; Lee, K.-W.; Rushman, P.; Brown, T. L. *Inorg. Chem.* **1986**, *25*, 1852.

0002-7863/89/1511-5983$01.50/0

transfers to the 18-electron metal complexes $Re(CO)_4L$ (L = PMe_3 and $P(O\text{-}i\text{-}Pr)_3$) forming $Re(CO)_4LX$ from an extensive list of alkyl halides.

In the gas phase, a variety of 17-electron metal carbonyl negative ions can be generated by dissociative electron attachment with the corresponding neutral metal carbonyl complexes (eq 3).

$$M(CO)_xL + e^- \rightarrow L(OC)_{x-1}M^{\bullet -} + CO \quad (3)$$

Nine of the metal complex negative ions chosen for the present study were $(OC)_4MX^{\bullet -}$ (M = Re or Mn and X = Cl or Br), $(\eta^3\text{-}C_3H_5)(OC)_3M^{\bullet -}$ (M = Re or Mn), $(OC)_5Cr^{\bullet -}$, $(OC)_4Fe^{\bullet -}$, and $(OC)_3Ni^{\bullet -}$. The formally 15-electron complexes $(OC)_3MnX^{\bullet -}$ (X = Br or Cl) were included in this study since they were generated along with the corresponding $(OC)_4MnX^{\bullet -}$ complexes by dissociative electron attachment on $Mn(CO)_5X$.

In a preliminary report of the reactions of $(OC)_4Fe^{\bullet -}$ with polyhalomethanes, formation of the $(OC)_4FeX^-$ products (and in two cases with CF_3X, $(OC)_2Fe(X)(CF_3)^{\bullet -}$ products) were accommodated by initial halogen-atom abstraction (eq 1).[9] The noted absence of reaction between $(OC)_4Fe^{\bullet -}$ with simple alkyl halides[9] has been verified;[10] the same conclusion was reached for $(OC)_5Cr^{\bullet -}$ and $(OC)_2Co(NO)^{\bullet -}$.[10] The present study was carried out to test the halogen-atom abstraction mechanistic hypothesis. Although phosphine and phosphite ligands were not represented in the 11 metal complex anion radicals, it was felt that the diversity of structures and metals available would be mechanistically significant.

Experimental Section

The flowing afterglow (FA) apparatus used in these studies has been described.[11,12] Briefly, a fast flow of helium buffer gas (P_{He} = 0.5 Torr, $\bar{v}$ = 80 m s^{-1}, 298 K) was established and maintained in the ≈1.5-m-long flow tube, and the electron gun located in the upstream end of the tube was turned on. Just downstream of the electron gun, the neutral metal carbonyl was continuously leaked into the flow. Dissociative attachment of thermal or near-thermal energy electrons occurred and gave the transition-metal complex negative ions of interest according to eq 3. The initially formed excited metal complex negative ions were then cooled to their vibrational ground states by multiple collisions with the helium buffer gas in the next 75 cm of the flow. At this point, the haloalkanes were added via a gas inlet, and the ion/molecule reactions occurred in the final 65 cm of the tube (distance between the latter inlet and the first sampling nose cone). The fast helium flow was sampled into a differentially pumped compartment (≈10^{-7} Torr) containing a quadrupole mass filter and electron multiplier, which continuously monitored the ion composition (starting and product) in the flow. Rate constants of the bimolecular ion/molecule reactions were determined under pseudo-first-order conditions by methods and calculations already given.[12] The neutral reaction products were assumed on the basis of mass balance and thermochemistry since they were not directly observed.

The preparations of $M(CO)_5X$ (M = Re, Mn; X = Cl, Br) were carried out according to the procedure of Eisch and King[13] by William Lewis. Alison Fleming prepared the samples of $(\eta^3\text{-}C_3H_5)Mn(CO)_4$[14] and $(\eta^3\text{-}C_3H_5)Re(CO)_4$.[15] The samples of $Fe(CO)_5$, $Cr(CO)_6$, and $Ni(CO)_4$ were obtained from commercial sources. The haloalkane gases were used as received from suppliers and were loaded into 5-L gas reservoirs after three freeze–pump–thaw cycles. Distilled, constant-boiling center cuts of the liquid haloalkanes were similarily treated.

Results

Dissociative electron attachment occurred with each of the nine 18-electron metal carbonyl complexes, $M(CO)_xL$, listed and produced the corresponding $L(OC)_x^{-1}M^{\bullet -}$ species (eq 3) shown in eq 4–12 with electron gun emission currents of <100 μA. The

$$Re(CO)_5Br + e^- \rightarrow \underset{m/z\ 375,\ 378,\ 380}{(OC)_4ReBr^{\bullet -}} + CO \quad (4)$$

$$Re(CO)_5Cl + e^- \rightarrow \underset{m/z\ 332,\ 334,\ 336}{(OC)_4ReCl^{\bullet -}} + CO \quad (5)$$

$$Mn(CO)_5Br + e^- \xrightarrow{0.75} \underset{m/z\ 246,\ 248}{(OC)_4MnBr^{\bullet -}} + CO \quad (6a)$$

$$\xrightarrow{0.25} \underset{m/z\ 218,\ 220}{(OC)_3MnBr^{\bullet -}} + 2CO \quad (6b)$$

$$Mn(CO)_5Cl + e^- \xrightarrow{0.60} \underset{m/z\ 202,\ 204}{(OC)_4MnCl^{\bullet -}} + CO \quad (7a)$$

$$\xrightarrow{0.40} \underset{m/z\ 174,\ 176}{(OC)_3MnCl^{\bullet -}} + 2CO \quad (7b)$$

$$(\eta^3\text{-}C_3H_5)Re(CO)_4 + e^- \xrightarrow{0.02} \underset{m/z\ 339,\ 341}{(C_3H_5)Re(CO)_4^{\bullet -}} \quad (8a)$$

$$\xrightarrow{0.98} \underset{m/z\ 311,\ 313}{(\eta^3\text{-}C_3H_5)Re(CO)_3^{\bullet -}} + CO \quad (8b)$$

$$(\eta^3\text{-}C_3H_5)Mn(CO)_4 + e^- \rightarrow \underset{m/z\ 180}{(\eta^3\text{–}C_3H_5)Mn(CO)_3^{\bullet -}} + CO \quad (9)$$

$$Cr(CO)_6 + e^- \rightarrow \underset{m/z\ 192}{(OC)_5Cr^{\bullet -}} + CO \quad (10)$$

$$Fe(CO)_5 + e^- \rightarrow \underset{m/z\ 169}{(OC)_4Fe^{\bullet -}} + CO \quad (11)$$

$$Ni(CO)_4 + e^- \rightarrow \underset{m/z\ 142,\ 144}{(OC)_3Ni^{\bullet -}} + CO \quad (12)$$

multiple m/z values for the negative ions given in eq 4–8 and 12 are the major isotope signals for these ion products, if those signals were >25% of the strongest signal in the isotope cluster.

The presence of the two ions $(OC)_{4,3}MnBr^{\bullet -}$ (eq 6) and $(OC)_{4,3}MnCl^{\bullet -}$ (eq 7) in the same flow experiments did not cause a problem in interpreting the halogen-atom-transfer data. Both ions reacted with similar rate constants and formed separate product ions differing by 28 amu (the CO ligand). Although $(OC)_3MnX^{\bullet -}$ where X = Br or Cl are formally 15-electron complexes, the similarities in their rate constants and product ions with those of $(OC)_4MnX^{\bullet -}$ (X = Br or Cl) suggest that the former complexes have 17-electron configurations on Mn with the halogen ligands serving as 3-electron donors. For these reasons, the kinetic and product data for the reactions of $(OC)_3MnBr^{\bullet -}$ and $(OC)_3MnCl^{\bullet -}$ with RX molecules are included in the present study.

Addition of measured concentrations of the haloalkane [RX] to the separate flows containing the $L(OC)_{x-1}M^{\bullet -}$ negative ions gave excellent pseudo-first-order decay plots (log ($L(OC)_{x-1}M^{\bullet -}$) signal) vs increasing [RX]) with correlation coefficients of >0.99. The bimolecular rate constants, k_{total}, listed in Tables I–XI are averages of duplicate determinations at P_{He} = 0.5 and 1.0 Torr where no P_{He} effect was noted.[16] While our ability to duplicate rate constants is <±10% of the average values given, the errors due to systematic uncertainties in calibrations suggest that their accuracy for external comparisons is ±20%. The FA allows determination of rate constants for reactions that occur at the collision limit ($k_{total} = k_{ADO}$[17] ≈ 10^{-9} cm^3 $molecule^{-1}$ s^{-1}) with the lower limit of $k_{total} = 10^{-13}$ cm^3 $molecule^{-1}$ s^{-1}.

Branching fractions for two or more primary product forming reaction channels have errors of ±4% absolute of the average values given and are corrected for any secondary reactions. Unless otherwise noted, the rate constants and branching fractions did

(9) McDonald, R. N.; Schell, P. L.; McGhee, W. D. *Organometallics* **1984**, *3*, 182.
(10) McElvany, S. W.; Allison, J. *Organometallics* **1986**, *5*, 416.
(11) McDonald, R. N.; Chowdhury, A. K. *J. Am. Chem. Soc.* **1985**, *107*, 4123.
(12) McDonald, R. N.; Chowdhury, A. K.; Setser, D. W. *J. Am. Chem. Soc.* **1980**, *102*, 6491.
(13) Eisch, J. J.; King, R. B. *Organometallic Synthesis*; Academic Press: New York, 1965; Vol. 1.
(14) Gibson, D. H.; Hsu, W. L.; Lin, D. S. *J. Organomet. Chem.* **1979**, *172*, C7.
(15) Ablel, E. W.; Moorhouse, S. J. *J. Chem. Soc., Dalton Trans.* **1973**, 1706.

(16) An error in a constant in the program used to calculate the ion–molecule bimolecular rate constants, k_{total}, was recently discovered which increases the rate constants given in the Ph.D. theses of M. T. Jones (KSU, 1987) and P. L. Schell (KSU, 1986) by 14.8%. The rate constants listed in this paper are corrected for this error.
(17) Su, T.; Bowers, M. T. In *Gas Phase Ion Chemistry*; Bowers, M. T.; Ed.; Academic Press: New York, 1979; Vol. 1, Chapter 3.

Table I. Summary of Kinetic and Product Data for the Reactions of $(OC)_4ReBr^{\bullet-}$ with Alkyl Halides

rxn no.	alkyl halide	product ion [+ assumed neutral(s)]	branching fraction[a]	k_{total},[b] cm^3 $molecule^{-1}$ s^{-1}	k_{ADO},[c] cm^3 $molecule^{-1}$ s^{-1}	rxn efficiency[d]
1a	CCl_4	$(OC)_4ReBrCl^-$ [+$^\bullet CCl_3$]	0.87	1.6×10^{-10}	7.2×10^{-10}	0.22
1b		$(OC)_3ReBrCl^-$ [+CO + $^\bullet CCl_3$]	0.13			
2	$CHCl_3$	$(OC)_4ReBrCl^-$ [+$^\bullet CHCl_2$]	1.00	1.1×10^{-12}	8.4×10^{-10}	0.0014
3	CH_2Cl_2	no reaction		$<10^{-13}$		
4	CH_3Cl	no reaction		$<10^{-13}$		
5	CCl_3CH_3	$(OC)_4ReBrCl^-$ [+$^\bullet CCl_2CH_3$]	1.00	3.1×10^{-12}	1.0×10^{-9}	0.0031
6	CCl_2FCClF_2	$(OC)_4ReBrCl^-$ [+$^\bullet C_2Cl_2F_3$]	1.00	4.1×10^{-11}		
7	CCl_3F	$(OC)_4ReBrCl^-$ [+$^\bullet CCl_2F$]	1.00	3.9×10^{-11}	7.4×10^{-10}	0.053
8	CCl_2F_2	$(OC)_4ReBrCl^-$ [+$^\bullet CClF_2$]	1.00	5.5×10^{-13}	7.3×10^{-10}	0.00075
9	$CClF_3$	no reaction		$<10^{-13}$		
10	CH_3Br	no reaction		$<10^{-13}$		
11	CF_3Br	$(OC)_4ReBr_2^-$ [+$^\bullet CF_3$]	1.00	1.1×10^{-10}	5.9×10^{-10}	0.20
12a	CCl_3Br	$(OC)_4ReBr_2^-$ [+$^\bullet CCl_3$]	0.51	3.2×10^{-10}	7.8×10^{-10}	0.41
12b		$(OC)_3ReBr_2^-$ [+CO + $^\bullet CCl_3$]	0.36			
12c		$(OC)_4ReBrCl^-$ [+$^\bullet CCl_2Br$]	0.13			
13	CH_3I	$(OC)_4ReBrI^-$ [+$^\bullet CH_3$]	1.00	9.8×10^{-12}	1.2×10^{-9}	0.0082
14	CF_3I	$(OC)_4ReBrI^-$ [+$^\bullet CF_3$]	1.00	4.8×10^{-10}	6.8×10^{-10}	0.71

[a] Errors in these branching fractions are ±4% absolute from the average values given. [b] k_{total}'s are averages of two determinations at $P_{He} = 0.5$ and 1.0 Torr. The errors in these values are <±10% of these averages. [c] Calculated collision limited rate constants using the average dipole orientation theory (ADO).[16] [d] Reaction efficiency is the fraction of collisions that result in reaction; k_{total}/k_{ADO}.

Table II. Summary of Kinetic and Product Data for the Reactions of $(OC)_4ReCl^{\bullet-}$ with Alkyl Halides

rxn no.	alkyl halide	product ion [+ assumed neutral(s)]	branching fraction[a]	k_{total},[b] cm^3 $molecule^{-1}$ s^{-1}	k_{ADO},[c] cm^3 $molecule^{-1}$ s^{-1}	rxn efficiency[d]
1a	CCl_4	$(OC)_4ReCl_2^-$ [+$^\bullet CCl_3$]	0.72	1.7×10^{-10}	7.4×10^{-10}	0.23
1b		$(OC)_3ReCl_2^-$ [+CO + $^\bullet CCl_3$]	0.28			
2	$CHCl_3$	$(OC)_4ReCl_2^-$ [+$^\bullet CCl_3$]	1.00	1.3×10^{-12}	8.5×10^{-10}	0.0015
3	CH_2Cl_2	no reaction		$<10^{-13}$		
4	CH_3Cl	no reaction		$<10^{-13}$		
5	CCl_3CH_3	$(OC)_4ReCl_2^-$ [$^\bullet CCl_2CH_3$]	1.00	3.2×10^{-12}	1.1×10^{-9}	0.0029
6	CCl_2FCClF_2	$(OC)_4ReCl_2^-$ [+$^\bullet C_2Cl_2F_3$]	1.00	4.2×10^{-11}		
7	CCl_3F	$(OC)_4ReCl_2^-$ [+$^\bullet CCl_2F$]	1.00	4.7×10^{-11}	7.6×10^{-10}	0.062
8	CCl_2F_2	$(OC)_4ReCl_2^-$ [+$^\bullet CClF_2$]	1.00	1.4×10^{-13}	7.5×10^{-10}	0.00018
9	$CClF_3$	no reaction		$<10^{-13}$		
10	CH_3Br	no reaction		$<10^{-13}$		
11	CF_3Br	$(OC)_4ReClBr^-$ [+$^\bullet CF_3$]	1.00	1.5×10^{-10}	6.0×10^{-10}	0.25
12	CH_3I	$(OC)_4ReClI^-$ [+$^\bullet CH_3$]	1.00	1.3×10^{-11}	1.2×10^{-9}	0.011
13	CF_3I	$(OC)_4ReClI^-$ [+$^\bullet CF_3$]	1.00	3.9×10^{-10}	6.9×10^{-10}	0.57

[a-d] See Table I.

not change outside of experimental errors when P_{He} was changed from 0.5 to 1.0 Torr.

Discussion

The thermodynamic data ($D°$(R–X),[18,19] EA,[20] and $\Delta H_f°$ [21,22]) for the haloalkanes used in the following sections are listed in Table XII. The rate constants for attachment of thermal energy electrons (thermal electron attachment, k_{TEA}) to the alkyl halides[23-26] are included in Table XII. The latter k_{TEA}'s are determined by several methods including electron capture from thermal energy electron swarms.

Some General Observations of the Results. For several of the fast halogen-atom-transfer reactions of the $L(OC)_{x-1}M^{\bullet-}$ complexes with neutrals, such as CCl_4, and in *all* of the reactions between $(OC)_3Ni^{\bullet-}$ and the haloalkanes (Table XI), two product ions, $L(OC)_{x-1}MX^-$ and $L(OC)_{x-2}MX^-$, were generated. We suggest that the relative branching fractions arise from the amount of excess vibrational energy present in $[L(OC)_{x-1}MX^-]^*$ following halogen-atom transfer (eq 13 and 14). For transfer of the same

$$L(OC)_{x-1}M^{\bullet-} + RX \rightarrow [L(OC)_{x-1}MX^-]^* + {}^\bullet R \quad (13)$$

$$[L(OC)_{x-1}MX^-]^* \xrightarrow{He} \begin{cases} L(OC)_{x-1}MX^- \\ L(OC)_{x-2}MX^- + CO \end{cases} \quad (14)$$

halogen atom to $(OC)_3Ni^{\bullet-}$ from a series of RX molecules, the excess energy in $[(OC)_3NiX^-]^*$ depends on the difference ($D°$(Ni–X) – $D°$(R–X)) and the partitioning of the energy between the two products, $^\bullet R$ and $(OC)_3NiX^-$.

It is interesting that the $(OC)_2NiX^-$ product ion formed in these generally fast reactions fail to react further with the excess RX molecules present in the flow. These metal complex negative ion products formally have 16-electron configurations about the metal center *if* the halogen is counted as a 1-electron donor ligand. Other 16-electron metal complex negative ions (e.g., $(OC)_3Co^-$ and $(OC)_4Mn^-$) react with most of the haloalkanes listed in Table XII at nearly the collision limit.[27] These results lead us to conclude that the $(OC)_2NiX^-$ products are, in fact, 18-electron complex negative ions with the halogen ligands functioning as 3-electron donors. This same type of M=X multiple bonding was considered to be operating in $(OC)_3MnX^{\bullet-}$ (X = Br or Cl) to account for the similarities in their rates of halogen-atom transfer from RX

(18) McMillen, D. F.; Golden, D. M. *Annu. Rev. Phys. Chem.* **1982**, *33*, 493.
(19) Weissman, M.; Benson, S. W. *J. Phys. Chem.* **1983**, *87*, 243.
(20) Christodoulides, A. A.; McCorkle, D. L.; Christophorou, L. G. In *Electron-Molecule Interactions and Their Applications*; Christophorou, L. G., Ed.; Academic Press: New York, 1984; Vol. 2, Chapter 6.
(21) Lias, S. G.; Karpas, Z.; Liebman, J. F. *J. Am. Chem. Soc.* **1985**, *107*, 6089.
(22) Cox, J. D.; Pilcher, G. *Thermochemistry of Organic and Organometallic Compounds*; Academic Press: New York, 1970.
(23) For a review and list of thermal electron attachment rate constants through 1983, see: Christophorou, L. G. In *Electron-Molecule Interactions and their Applications*; Christophorou, L. G., Ed.; Academic Press: New York, 1984; Vol. 1, Chapter 6.
(24) Smith, D.; Adams, N. G.; Alge, E. *J. Phys. B: At. Mol. Phys.* **1984**, *17*, 461, 3827.
(25) Fessenden, R. W.; Bansal, K. M. *J. Chem. Phys.* **1970**, *53*, 3468.
(26) McCorle, et al. (McCorkle, D. L.; Christodoulides, A. A.; Christophorou, L. G.; Szamrej, I. *J. Chem. Phys.* **1980**, *72*, 4049) reported the k_{TEA} for CCl_3F, but later corrected the compound to be CCl_2FCClF_2 (*Ibid.* **1982**, *76*, 753).
(27) Jones, M. T. Ph.D. Thesis, Kansas State University, 1987.

Table III. Summary of Kinetic and Product Data for the Reactions of $(OC)_4MnBr^{\bullet-}$ with Alkyl Halides

rxn no.	alkyl halide	product ion [+ assumed neutral(s)]	branching fraction[a]	k_{total},[b] cm^3 molecule^{-1} s^{-1}	k_{ADO},[c] cm^3 molecule^{-1} s^{-1}	rxn efficiency[d]
1	CCl_4	$(OC)_4MnBrCl^-$ [+$^\bullet CCl_3$]	1.00	2.9×10^{-13}	7.7×10^{-10}	0.00037
2	$CHCl_3$	no reaction		$<10^{-13}$		
3	CH_2Cl_2	no reaction		$<10^{-13}$		
4	CH_3Cl	no reaction		$<10^{-13}$		
5	CCl_3CH_3	no reaction		$<10^{-13}$		
6	CCl_2FCClF_2	no reaction		$<10^{-13}$		
7	CCl_3F	no reaction		$<10^{-13}$		
8	CCl_2F_2	no reaction		$<10^{-13}$		
9	$CClF_3$	no reaction		$<10^{-13}$		
10	CH_3Br	no reaction		$<10^{-13}$		
11	CF_3Br	$(OC)_4MnBr_2^-$ [+$^\bullet CF_3$]	1.00	1.3×10^{-13}	7.0×10^{-10}	0.00018
12	CCl_3Br	$(OC)_4MnBr_2^-$ [+$^\bullet CCl_3$]	1.00	2.4×10^{-10}	7.6×10^{-10}	0.32
13	CH_3I	no reaction		$<10^{-13}$		
14	CF_3I	$(OC)_4MnBrI^-$ [+$^\bullet CF_3$]	1.00	3.1×10^{-10}	7.4×10^{-10}	0.42

[a-d] See Table I.

Table IV. Summary of Kinetic and Product Data for the Reactions of $(OC)_3MnBr^{\bullet-}$ with Alkyl Halides

rxn no.	alkyl halide	product ion [+ assumed neutral(s)]	branching fraction[a]	k_{total},[b] cm^3 molecule^{-1} s^{-1}	k_{ADO},[c] cm^3 molecule^{-1} s^{-1}	rxn efficiency[d]
1	CCl_4	$(OC)_3MnBrCl^-$ [+$^\bullet CCl_3$]	1.00	5.3×10^{-12}	7.9×10^{-10}	0.0067
2	$CHCl_3$	no reaction		$<10^{-13}$		
3	CH_2Cl_2	no reaction		$<10^{-13}$		
4	CH_3Cl	no reaction		$<10^{-13}$		
5	CCl_3CH_3	$(OC)_3MnBrCl^-$ [+$^\bullet CCl_2CH_3$]	1.00	3.7×10^{-13}	1.1×10^{-9}	0.00034
6	CCl_2FCClF_2	no reaction	1.00	$<10^{-13}$		
7	CCl_3F	$(OC)_3MnBrCl^-$ [+$^\bullet CCl_2F$]	1.00	1.1×10^{-13}	8.0×10^{-10}	0.00014
8	CCl_2F_2	no reaction		$<10^{-13}$		
9	$CClF_3$	no reaction		$<10^{-13}$		
10	CH_3Br	no reaction		$<10^{-13}$		
11	CF_3Br	$(OC)_3MnBr_2^-$ [+$^\bullet CF_3$]	1.00	1.5×10^{-13}	7.0×10^{-10}	0.0021
12	CCl_3Br	$(OC)_3MnBr_2^-$ [+$^\bullet CCl_3$]	1.00	3.2×10^{-10}	7.8×10^{-10}	0.41
13	CH_3I	no reaction		$<10^{-13}$		
14	CF_3I	$(OC)_3MnBrI^-$ [+$^\bullet CF_3$]	1.00	3.1×10^{-10}	7.5×10^{-10}	0.41

[a-d] See Table I.

Table V. Summary of Kinetic and Product Data for the Reactions of $(OC)_4MnCl^{\bullet-}$ with Alkyl Halides

rxn no.	alkyl halide	product ion [+ assumed neutral(s)]	branching fraction[a]	k_{total},[b] cm^3 molecule^{-1} s^{-1}	k_{ADO},[c] cm^3 molecule^{-1} s^{-1}	rxn efficiency[d]
1	CCl_4	$(OC)_4MnCl_2^-$ [+$^\bullet CCl_3$]	1.00	4.9×10^{-13}	8.1×10^{-10}	0.00061
2	$CHCl_3$	no reaction		$<10^{-13}$		
3	CH_2Cl_2	no reaction		$<10^{-13}$		
4	CH_3Cl	no reaction		$<10^{-13}$		
5	CCl_3CH_3	no reaction		$<10^{-13}$		
6	CCl_2FCClF_2	no reaction		$<10^{-13}$		
7	CCl_3F	no reaction		$<10^{-13}$		
8	CCl_2F_2	no reaction		$<10^{-13}$		
9	$CClF_3$	no reaction		$<10^{-13}$		
10	CH_3Br	no reaction		$<10^{-13}$		
11	CF_3Br	$(OC)_4MnClBr^-$ [+$^\bullet CF_3$]	1.00	1.1×10^{-13}	7.1×10^{-10}	0.00016
12	CH_3I	no reaction		$<10^{-13}$		
13	CF_3I	$(OC)_4MnClI^-$	1.00	2.9×10^{-10}	7.5×10^{-10}	0.38

[a-d] See Table I.

Table VI. Summary of Kinetic and Product Data for the Reactions of $(OC)_3MnCl^{\bullet-}$ with Alkyl Halides

rxn no.	alkyl halide	product ion [+ assumed neutral(s)]	branching fraction[a]	k_{total},[b] cm^3 molecule^{-1} s^{-1}	k_{ADO},[c] cm^3 molecule^{-1} s^{-1}	rxn efficiency[d]
1	CCl_4	$(OC)_3MnCl_2^-$ [+$^\bullet CCl_3$]	1.00	3.9×10^{-12}	8.4×10^{-10}	0.0046
2	$CHCl_3$	no reaction		$<10^{-13}$		
3	CH_2Cl_2	no reaction		$<10^{-13}$		
4	CH_3Cl	no reaction		$<10^{-13}$		
5	CCl_3CH_3	no reaction		$<10^{-13}$		
6	CCl_2FCClF_2	no reaction		$<10^{-13}$		
7	CCl_3F	no reaction		$<10^{-13}$		
8	CCl_2F_2	no reaction		$<10^{-13}$		
9	$CClF_3$	no reaction		$<10^{-13}$		
10	CH_3Br	no reaction		$<10^{-13}$		
11	CF_3Br	$(OC)_3MnClBr^-$ [+$^\bullet CF_3$]	1.00	1.3×10^{-13}	7.0×10^{-10}	0.00018
12	CH_3I	no reaction		$<10^{-13}$		
13	CF_3I	$(OC)_3MnClI^-$ [+$^\bullet CF_3$]	1.00	2.9×10^{-10}	7.6×10^{-10}	0.38

[a-d] See Table I.

Table VII. Summary of Kinetic and Product Data for the Reactions of $(\eta^3\text{-}C_3H_5)Re(CO)_3^{\bullet-}$ with Alkyl Halides

rxn no.	alkyl halide	product ion [+ assumed neutral(s)]	branching fraction[a]	k_{total},[b] cm^3 molecule^{-1} s^{-1}	k_{ADO},[c] cm^3 molecule^{-1} s^{-1}	rxn efficiency[d]
1	CCl_4	$(\eta^3\text{-}C_3H_5)Re(CO)_3Cl^-$ [+$^\bullet CCl_3$]	1.00	4.1×10^{-10}	7.5×10^{-10}	0.55
2	CH_2Cl_2	$(\eta^3\text{-}C_3H_5)Re(CO)_3Cl^-$ [+$^\bullet CH_2Cl$]	1.00	1.6×10^{-12}	1.0×10^{-9}	0.0016
3	CH_3Cl	no reaction		$<10^{-13}$		
4	CF_3Cl	no reaction		$<10^{-13}$		
5	CH_3Br	no reaction		$<10^{-13}$		
6a	CH_3I	$(\eta^3\text{-}C_3H_5)Re(CO)_3I^-$ [+$^\bullet CH_3$]	0.12	1.6×10^{-10}	1.2×10^{-9}	0.13
6b		$(\eta^3\text{-}C_3H_5)Re(CO)_2I^-$ [+CO + $^\bullet CH_3$]	0.88			

[a-d] See Table I.

Table VIII. Summary of Kinetic and Product Data for the Reactions of $(\eta^3\text{-}C_3H_5)Mn(CO)_3^{\bullet-}$ with Alkyl Halides

rxn no.	alkyl halide	product ion [+ assumed neutral(s)]	branching fraction[a]	k_{total},[b] cm^3 molecule^{-1} s^{-1}	k_{ADO},[c] cm^3 molecule^{-1} s^{-1}	rxn efficiency[d]
1	CCl_4	$(\eta^3\text{-}C_3H_5)Mn(CO)_3Cl^-$ [+$^\bullet CCl_3$]	1.00	3.6×10^{-10}	8.3×10^{-10}	0.43
2	CH_2Cl_2	no reaction		$<10^{-13}$		
3	CH_3Cl	no reaction		$<10^{-13}$		
4	CF_3Cl	no reaction		$<10^{-13}$		
5	CH_3Br	no reaction		$<10^{-13}$		
6	CH_3I	$(\eta^3\text{-}C_3H_5)Mn(CO)_3I^-$ [+$^\bullet CH_3$]	1.00	6.3×10^{-12}	1.8×10^{-9}	0.0035
7	CF_3I	$(\eta^3\text{-}C_3H_5)Mn(CO)_3I^-$ [+$^\bullet CF_3$]	1.00	5.6×10^{-10}	8.1×10^{-10}	0.69

[a-d] See Table I.

Table IX. Summary of Kinetic and Product Data for the Reactions of $(OC)_5Cr^{\bullet-}$ with Alkyl Halides

rxn no.	alkyl halide	product ion [+ assumed neutral(s)]	branching fraction[a]	k_{total},[b] cm^3 molecule^{-1} s^{-1}	k_{ADO},[c] cm^3 molecule^{-1} s^{-1}	rxn efficiency[d]
1a	CCl_4	$(OC)_5CrCl^-$ [+$^\bullet CCl_3$]	0.95	2.5×10^{-10}	8.1×10^{-10}	0.31
1b		$(OC)_4CrCl^-$ [+CO + $^\bullet CCl_3$]	0.05			
2	$CHCl_3$	$(OC)_5CrCl^-$ [+$^\bullet CHCl_2$]	1.00	6.1×10^{-12}	9.3×10^{-10}	0.0065
3	CH_2Cl_2	no reaction		$<10^{-13}$		
4	CH_3Cl	no reaction		$<10^{-13}$		
5	CCl_3CH_3	$(OC)_5CrCl^-$ [+$^\bullet CCl_2CH_3$]	1.00	8.0×10^{-12}	1.1×10^{-9}	0.0073
6	CCl_2FCClF_2	$(OC)_5CrCl^-$ [+$^\bullet C_2Cl_2F_3$]	1.00	1.7×10^{-10}		
7	CCl_3F	$(OC)_5CrCl^-$ [+$^\bullet CCl_2F$]	1.00	1.1×10^{-10}	8.3×10^{-10}	0.14
8	CF_2Cl_2	$(OC)_5CrCl^-$ [+$^\bullet CF_2Cl$]	1.00	5.2×10^{-12}	8.0×10^{-10}	0.0065
9	CF_3Cl	no reaction		$<10^{-13}$		
10	CH_3Br	no reaction		$<10^{-13}$		
11	CF_3Br	$(OC)_5CrBr^-$ [+$^\bullet CF_3$]	1.00	2.1×10^{-10}	6.8×10^{-10}	0.30
12	CH_3I	$(OC)_5CrI^-$ [+$^\bullet CH_3$]	1.00	2.1×10^{-11}	9.9×10^{-10}	0.021
13	CF_3I	$(OC)_5CrI^-$ [+$^\bullet CF_3$]	1.00	6.3×10^{-10}	7.8×10^{-10}	0.81

[a-d] See Table I.

Table X. Summary of Kinetic and Product Data for the Reactions of $(OC)_4Fe^{\bullet-}$ with Alkyl Halides

rxn no.	alkyl halide	product ion [+ assumed neutral(s)]	branching fraction[a]	k_{total},[b] cm^3 molecule^{-1} s^{-1}	k_{ADO},[c] cm^3 molecule^{-1} s^{-1}	rxn efficiency[d]
1	CCl_4	$(OC)_4FeCl^-$ [+$^\bullet CCl_3$]	1.00	8.8×10^{-12}	8.4×10^{-10}	0.011
2	$CHCl_3$	no reaction		$<10^{-13}$		
3	CH_2Cl_2	no reaction		$<10^{-13}$		
4	CH_3Cl	no reaction		$<10^{-13}$		
5	CCl_3CH_3	no reaction		$<10^{-13}$		
6	CCl_2FCClF_2	no reaction		$<10^{-13}$		
7	CCl_3F	no reaction		$<10^{-13}$		
8	CCl_2F_2	no reaction		$<10^{-13}$		
9	CF_3Cl	no reaction		$<10^{-13}$		
10	CH_3Br	no reaction		$<10^{-13}$		
11a	CF_3Br	$(OC)_4FeBr^-$ [+$^\bullet CF_3$]	0.73	2.0×10^{-12}	7.0×10^{-10}	0.0028
11b		$(OC)_2Fe(Br)(CF_3)^{\bullet-}$ [+2CO]	0.27			
12	CCl_3Br	$(OC)_4FeBr^-$ [+$^\bullet CCl_3$]	1.00	2.6×10^{-10}	7.8×10^{-10}	0.34
13	CH_3I	no reaction		$<10^{-13}$		
14a	CF_3I	$(OC)_4FeI^-$ [+$^\bullet CF_3$]	0.88	5.3×10^{-10}	8.1×10^{-10}	0.65
14b		$(OC)_2Fe(I)(CF_3)^{\bullet-}$ [+2CO]	0.12			

[a-d] See Table I.

molecules as was observed with the respective 17-electron $(OC)_4MnX^-$ complexes.

The reactions of $(OC)_4Fe^{\bullet-}$ with CF_3X (X = Br or I) were the only ones where small amounts of the product negative ions incorporating the CF_3X molecule with loss of two CO ligands were formed along with the major product of halogen-atom transfer (reactions 11 and 13 in Table X). Our original interpretation of these results was that the excited complex **3** produced by halogen-atom transfer (independent of the mechanism) could competitively separate (a) or add the CF_3 radical (b) at either Fe[28] or a CO ligand (eq 15). Since similar oxidative insertions with

$$(OC)_4Fe^{\bullet-} + CF_3X \rightarrow [(OC)_4Fe^{\bullet-}/CF_3X]^* \rightarrow [(OC)_4FeX^-/{}^\bullet CF_3]^* \xrightarrow{a} (OC)_4FeX^- + {}^\bullet CF_3$$
$$\mathbf{3}$$
$$\xrightarrow{b} [(OC)_3Fe(C(=O)CF_3)^{\bullet-}]^* \text{ or } [(OC)_4Fe(X)(CF_3)^{\bullet-}]^* \rightarrow (OC)_2Fe(X)(CF_3)^{\bullet-} + 2CO \quad (15)$$

Table XI. Summary of Kinetic and Product Data for the Reactions of $(OC)_3Ni^{\bullet-}$ with Alkyl Halides

rxn no.	alkyl halide	product ion [+ assumed neutral(s)]	branching fraction[a]	k_{total},[b] cm^3 molecule^{-1} s^{-1}	k_{ADO},[c] cm^3 molecule^{-1} s^{-1}	rxn efficiency[d]
1a	CCl_4	$(OC)_3NiCl^-$ [+$^\bullet CCl_3$]	0.02	6.1×10^{-10}	9.1×10^{-10}	0.67
1b		$(OC)_2NiCl^-$ [+CO + $^\bullet CCl_3$]	0.98			
2a	$CHCl_3$	$(OC)_3NiCl^-$ [+$^\bullet CHCl_2$]	0.42	2.3×10^{-10}	1.3×10^{-9}	0.18
2b		$(OC)_2NiCl^-$ [+CO + $^\bullet CHCl_2$]	0.58			
3	CH_2Cl_2	no reaction		$<10^{-13}$		
4	CH_3Cl	no reaction		$<10^{-13}$		
5a	CCl_3F	$(OC)_3NiCl^-$ [+$^\bullet CCl_2F$]	0.13	4.4×10^{-10}	9.3×10^{-10}	0.47
5b		$(OC)_2NiCl^-$ [+CO + $^\bullet CCl_2F$]	0.87			
6a	CCl_2F_2	$(OC)_3NiCl^-$ [+$^\bullet CF_2Cl$]	0.76	1.8×10^{-10}	9.3×10^{-10}	0.20
6b		$(OC)_2NiCl^-$ [+CO + $^\bullet CF_2Cl$]	0.24			
7	$CClF_3$	no reaction		$<10^{-13}$		
8a	CH_3Br	$(OC)_3NiBr^-$ [+$^\bullet CH_3$]	0.69	7.2×10^{-12}	2.4×10^{-10}	0.030
8b		$(OC)_2NiBr^-$ [+CO + $^\bullet CH_3$]	0.31			
9a	CF_3Br	$(OC)_3NiBr^-$ [+$^\bullet CF_3$]	0.75	4.6×10^{-10}	7.2×10^{-10}	0.64
9b		$(OC)_2NiBr^-$ [+CO + $^\bullet CF_3$]	0.25			
10a	CF_3I	$(OC)_3NiI^-$ [+$^\bullet CF_3$]	0.20	7.7×10^{-10}	1.0×10^{-9}	0.77
10b		$(OC)_2NiI^-$ [+CO + $^\bullet CF_3$]	0.80			

[a-d] See Table II.

Table XII. Thermodynamic and Kinetic Data for the Alkyl Halides Used in This Study

alkyl halide	$D°$(C–X),[a] kcal mol^{-1}	EA,[b] kcal mol^{-1}	$\Delta H_f°$,[c] kcal mol^{-1}	k_{TEA},[d] cm^3 molecule^{-1} s^{-1}
R–Cl				
CCl_4	70.3[e]	46.0	−22.9	3.9×10^{-7}[g]
$CHCl_3$	79.2[e]	40.4	−24.7	4.4×10^{-9}[g]
CH_2Cl_2	82.8[e]	−28.3	−22.8	4.8×10^{-12}[h]
CH_3Cl	83.6[e]	−79.35	−19.3	$<2 \times 10^{-15}$
CCl_3CH_3	70.2			1.6×10^{-8}
CCl_2FCClF_2				3.9×10^{-8}[i]
CCl_3F	73.0	25.3	−64.1	2.6×10^{-7}[g]
CCl_2F_2	76.0	9.2	−114.1	3.2×10^{-9}[g]
$CClF_3$	86.2	−9.2	−166.0	1.8×10^{-13}[g]
R–Br				
CH_3Br	70.9	−10.58	−9.1[f]	6.0×10^{-12}[g]
CF_3Br	70.6	20.93	−155.0[f]	1.6×10^{-8}[g]
CCl_3Br	55.3		−9.3[f]	
R–I				
CH_3I	57.2	4.6	3.4[f]	1.2×10^{-7}[g]
CF_3I	55.0	36.1	−140.6[f]	

[a] Reference 18. [b] Reference 20. [c] Reference 21. [d] Reference 23. [e] Reference 19. [f] Reference 22. [g] Reference 24. [h] Reference 25. [i] Reference 26.

a two-electron change at the metal center were not observed with the other metal complex negative ions in this study, the specificity for these reactions with the Fe complex suggests that the six-coordinate negative ion $[(OC)_4Fe(X)(CF_3)^{\bullet-}]^*$ is the most likely intermediate.[28] If the larger $D°(C–CF_3)$ compared to $D°(C–CCl_3)$ by ≈11 kcal mol^{-1} carries over to the Fe–CX_3 bond energies, this could explain why the reactions with $CBrCl_3$ and CCl_4 failed to yield oxidative insertion product ions.

Mechanistic Considerations. A. Evidence against the Halogen-Atom-Abstraction Mechanism. As pointed out in the introduction, our original mechanistic hypothesis was that halogen-atom abstraction was occurring in the halogen-atom-transfer reactions between $(OC)_4Fe^{\bullet-}$ and several CY_3X molecules.[9] If this hypothesis was established, we could determine a variety of M–X bond energies in these $L(OC)_{x-1}MX^-$ anions from bracketing studies assuming that endothermic halogen–atom transfers were not observed. $D°(L(OC)_{x-1}M^-–X)$ values determined by bracketing reactions depend on the matching of this dissociation energy with the $D°$(R–X) for a series of alkyl halides as closely as possible and is shown in the thermochemical cycle in eq 16. As the

$$L(OC)_{x-1}M^{\bullet-} + RX \longrightarrow L(OC)_{x-1}MX^- + {}^\bullet R \qquad (16)$$

$$D°(R–X) \searrow \quad \nearrow -D°(L(OC)_{x-1}M^-–X)$$

$$L(OC)_{x-1}M^{\bullet-} + {}^\bullet X + {}^\bullet R$$

(28) Petz (Petz, W. *Organometallics* **1983**, *2*, 1044) reported evidence for a neutral six-coordinate Fe species.

Table XIII. $D°$(C–X) of Several Haloalkanes and the Rate Constants for Their Reactions with $(OC)_5Cr^{\bullet-}$, $(OC)_4ReBr^{\bullet-}$, and $(OC)_4ReCl^{\bullet-}$

RX	$D°$(C–X),[a] kcal mol^{-1}	k_{total}, cm^3 molecule^{-1} s^{-1} $(OC)_5Cr^{\bullet-}$[b]	$(OC)_4ReBr^{\bullet-}$[c]	$(OC)_4ReCl^{\bullet-}$[d]
CF_3I	55.0	6.3×10^{-10}	4.8×10^{-10}	3.9×10^{-10}
CH_3I	57.2	2.1×10^{-11}	9.8×10^{-12}	1.3×10^{-11}
CF_3Br	70.6	2.1×10^{-10}	1.1×10^{-10}	1.5×10^{-10}
CH_3Br	70.9	$<10^{-13}$	$<10^{-13}$	$<10^{-13}$
CCl_4	70.3	2.5×10^{-10}	1.6×10^{-10}	1.7×10^{-10}
CCl_3CH_3	70.2	8.0×10^{-12}	3.1×10^{-12}	3.2×10^{-12}

[a] From Table XII. [b] From Table IX. [c] From Table I. [d] From Table II.

halogen-atom-abstraction reaction approaches thermal neutrality, the rate constant should decrease. However, if the electron-transfer mechanism were to operate, such determined M–X bond energies might represent only lower limits,[29] with some other property of RX supplying the bottleneck. With either mechanism, the reaction energetics are controlled by the two R–X and M–X bond dissociation energies assuming $\Delta S = 0$. Since the reactivity data with $(OC)_4Fe^{\bullet-}$ was limited to only a few halomethanes undergoing reaction, it was essential to examine the ion/molecule reactions of a number of other 17-electron $L(OC)_{x-1}M^{\bullet-}$ complexes.

In Table XIII the kinetic data for the metal complex negative ions $(OC)_5Cr^{\bullet-}$, $(OC)_4ReBr^{\bullet-}$, and $(OC)_4ReCl^{\bullet-}$ are listed along with the $D°$(C–X) values for six selected haloalkanes with which they reacted to yield the products of halogen-atom transfer. These three metal complex negative ions had the more extensive lists of observed reactions with the haloalkanes. The selected alkyl halides demonstrated the cases where the pairs involved in transferring the same halogen atom had quite similar C–X bond energies. We observe *no* correlation of the rate constants for halogen-atom transfer with the C–X bond dissociation energies. This is most clearly seen in the Br- and Cl-atom transfer reactions in Table XIII.

While the majority of the halogen-atom-transfer reactions of $(OC)_3Ni^{\bullet-}$ are fast (Table XI), the rate constants for the reactions with CH_3Br and CF_3Br (similar $D°$(C–Br)) differ by a factor of 50. In the reactions of $(OC)_{3,4}MnBr^{\bullet-}$ (Tables III and IV), $(OC)_{3,4}MnCl^{\bullet-}$ (Tables V and VI), and $(OC)_4Fe^{\bullet-}$ (Table X) with CF_3I and CH_3I (same $D°$(C–I)), the reactions with CF_3I occurred with high reaction efficiencies ($k_{total}/k_{ADO} > 0.3$), but no reactions were observed with CH_3I (reaction efficiencies <0.0001). *The sum of these comparisons leads us to conclude that the halogen-atom-abstraction mechanism shown in eq 1 is not operating in these halogen-atom-transfer reactions.*

B. Electron-Transfer Mechanism. Having eliminated the halogen-atom-abstraction mechanism for these halogen-atom transfer reactions between the 17-electron $L(OC)_{x-1}M^{\bullet-}$ negative

(29) Squires, R. R. *Chem. Rev.* **1987**, *87*, 623.

Table XIV. EA and $D°(R-Cl^{•-})$ of Selected Chloroalkanes and the Rate Constants for Their Chlorine-Atom-Transfer Reactions with $(OC)_5Cr^{•-}$ and $(OC)_4ReBr^{•-}$

RX	EA,[a] kcal mol^{-1}	k_{total}, cm^3 molecule^{-1} s^{-1} $(OC)_5Cr^{•-}$[b]	k_{total}, cm^3 molecule^{-1} s^{-1} $(OC)_4ReBr^{•-}$[c]	$D°(R-Cl^{•-})$,[d] kcal mol^{-1}
CCl_4	46.0	2.5×10^{-10}	1.6×10^{-10}	31.5
$CHCl_3$	40.4	6.1×10^{-12}	1.1×10^{-12}	34.8
$CFCl_3$	25.3	1.1×10^{-10}	3.9×10^{-11}	13.5
CF_2Cl_2	9.2	5.2×10^{-12}	5.5×10^{-13}	0.4
CH_2Cl_2	−28.3	$<10^{-13}$	$<10^{-13}$	−30.3

[a] From Table XII. [b] From Table IX. [c] From Table I. [d] Calculated as described in the text.

ion complexes and the haloalkanes, we will now consider the electron-transfer mechanism. Since X^- or $RX^{•-}$ for those haloalkanes that yield stable anion radicals (e.g., $CF_3I^{•-}$) in the flowing afterglow are not observed, we believe that the electron transfer must occur in the excited ion/neutral collision complex **4** in eq 17. Such collision complexes are bound by 10–20 kcal mol^{-1} from

$$L(OC)_{x-1}M^{•-} + RX \overset{a}{\rightleftharpoons} \underset{\mathbf{4}}{[L(OC)_{x-1}M^{•-}/RX]^*} \overset{b}{\rightleftharpoons} \underset{\mathbf{5}}{[L(OC)_{x-1}M/RX^{•-}]^*} \xrightarrow{c} \underset{\mathbf{6}}{[L(OC)_{x-1}MX^-/R^•]^*} \xrightarrow{d} L(OC)_{x-1}MX^- + R^• \quad (17)$$

the attractive ion–dipole and ion–induced dipole interactions. This energy can help to overcome endothermic electron transfer. In complex **5**, the neutral metal complex $L(OC)_{x-1}M$ has a 16-electron metal electronic configuration and should readily bind X^- from $RX^{•-}$ to yield complex 6. Separation of 6 would then yield the observed product negative ions $L(OC)_{x-1}MX^-$.

We then began a search for thermodynamic or kinetic parameters that would correlate the kinetic data in Tables I–XI. Identification of such parameters would be useful in characterizing the reaction mechanism and could add significantly to our understanding of the process.

1. Absence of Correlation of Kinetic Data with the Thermodynamic Electron Affinities of the RX Molecules. The thermodynamic electron affinities (EA_T) of the haloalkanes are the differences in the energies of the RX molecules and the electron at rest at infinity separation and the $RX^{•-}$ with both the RX and $RX^{•-}$ species in their ground electronic, vibrational, and rotational states. Thus, $EA_T(RX)$ is an adiabatic property of RX.

A trend is observed of decreasing rate constants for a given $L(OC)_{x-1}M^{•-}$ complex as the EA_T of the haloalkane decreases. However, the breakdown in the quantitative nature of this correlation becomes apparent when the more extensive reaction lists for $(OC)_5Cr^{•-}$ and $(OC)_4ReX^{•-}$ (X = Br or Cl) are compared. In Table XIV, the rate constants for the chlorine-atom-transfer reactions between $(OC)_5Cr^{•-}$ and $(OC)_4ReBr^{•-}$ (similar to that of $(OC)_4ReCl^{•-}$) with several RCl molecules are listed along with the $EA_T(RCl)$ values for these haloalkanes. In each of these two columns of rate constants, the metal complex negative ion and the product $D°(M^-–Cl)$ are constants. Here we note the uncorrelated behavior of the k_{total} vs $EA_T(RCl)$ data for $CHCl_3$, $CFCl_3$, and CF_2Cl_2 using the data for CCl_4 and CH_2Cl_2 as upper and lower boundaries.

2. Absence of Correlation of the Kinetic Data with the C–X Bond Energies of the $RX^{•-}$ Species. In the general mechanistic scheme described for these halogen-atom-transfer reactions in eq 17, step c involves the transfer of X^- from $RX^{•-}$ to the 16-electron metal complex $L(OC)_{x-1}M$ in complex **5**, yielding complex 6. The energetics and, thus, the rates of step c depend on the bond energies of C–X bonds in $RX^{•-}$ ($D°(R-X^{•-})$) and the M–X bond in $L(OC)_{x-1}M-X^-$. To determine if this step could have a major influence on the observed rate constants, k_{total}, of these halogen-atom-transfer reactions, we calculated the $D°(R-X^{•-})$ of the *ground-state* molecular anion radicals $RX^{•-}$ from the relationship $D°(R-X^{•-}) = \Delta H_f°(R^•) + \Delta H_f°(X^-) - \Delta H_f°(RX^{•-})$, where $\Delta H_f°(R^•) = \Delta H_f°(RX) + D°(R-X) - \Delta H_f°(X^•)$ and $\Delta H_f°(RX^{•-}) = \Delta H_f°(RX) - EA_T(RX)$.

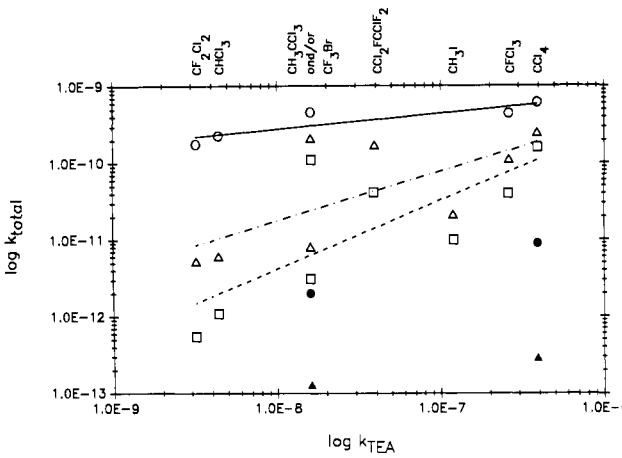

Figure 1. Plot of log k_{total} for the reactions of $(OC)_3Ni^{•-}$ (○), $(OC)_5Cr^{•-}$ (△), $(OC)_4ReBr^{•-}$ (□), $(OC)_4Fe^{•-}$ (●), and $(OC)_4MnBr^{•-}$ (▲) with the RX molecules listed along the top axis vs the log k_{TEA}'s for these haloalkanes. Correlation lines (solid for $(OC)_3Ni^{•-}$, –·– for $(OC)_5Cr^{•-}$, and – – – for $(OC)_4ReBr^{•-}$) include all of the data points.

For a given $L(OC)_{x-1}M^{•-}$ metal complex and the same halogen-atom transferred, $D°(L(OC)_{x-1}M-X^-)$ will be constant. The calculated $D°(R-Cl^{•-})$ values and the kinetic data for chlorine-atom transfers to $(OC)_5Cr^{•-}$ and $(OC)_4ReBr^{•-}$ are listed in Table XIV. Here the absence of correlation of the kinetic data is obvious. Therefore, step c does not contribute to the k_{total}'s in the present halogen-atom-transfer reactions.

3. Correlation of the Kinetic Data with the Rate Constants and Activation Energies for Thermal Electron Attachment to the Haloalkanes. Reactions of the alkali-metal atoms with alkyl halides to yield the metal halide molecules have been shown to occur by an electron-transfer ("harpoon") mechanism.[30-33] Polanyi noted that a correlation existed between the enthalpy change for the reaction of Na atoms with the alkyl chlorides giving NaCl and the radical $^•R$ and the rate constants for attachment of thermal energy electrons to the alkyl chlorides.[30] From this correlation, Polanyi concluded that an electron-transfer mechanism must be involved and that the halogen-transfer process was related to the *vertical electron affinities* of the alkyl halides.[34]

The thermal electron attachment rate constants, k_{TEA}, for the haloalkanes used in this study are listed in Table XII. We have selected the recently reported k_{TEA}'s determined by Smith et al.[24] for eight of the haloalkanes listed in Table XII, since they come from the same laboratory with a flowing afterglow–Langmuir probe apparatus. (A microwave cavity and discharge was placed in the upstream end of the flow tube for the production of electrons which were carried downstream with the buffer gas. The haloalkane could then be added to the flow, and the movable Langmuir probe was used to measure the electron, positive ion, and negative ion number densities.) The other four k_{TEA}'s were determined by different groups. For the more extensive kinetic data sets of $(OC)_4ReBr^{•-}$, $(OC)_4ReCl^{•-}$, and $(OC)_5Cr^{•-}$, good correlations exist for k_{total} vs the k_{TEA} values of the haloalkanes in Table XV. The single major deviation occurred for the chlorine-atom-transfer constant with the CCl_2FCClF_2 molecule where the only reported k_{TEA} value[26] predicted *smaller* k_{total}'s (by a factor of ≈10) than were observed. The present kinetic data and correlation suggest that k_{TEA} for CCl_2FCClF_2 should be similar to that for $CFCl_3$.

The plot of the rate constants for halogen-atom transfer vs k_{TEA} for the haloalkanes in Figure 1 includes the larger data sets of

(30) Polanyi, M. *Atomic Reactions*; Williams: Northgate, London, 1932.
(31) Herschbach, D. R. *Adv. Chem. Phys.* **1966**, *10*, 319.
(32) Davidouits, P.; McFadden, D. L. *Alkali Halide Vapors: Structure, Spectra, and Reaction Dynamics*; Academic Press: New York, 1979.
(33) Brooks et al. (Carman, H. S.; Harland, P. W.; Brooks, P. R. *J. Phys. Chem.* **1986**, *90*, 944) recently reported the reaction of K atom wtih oriented CF_3Br.
(34) This mechanism also applies to the quenching reactions of metastable states of the rare gases and various other atoms with RX molecules; see: Zhang, F. M.; Oba, D.; Setser, D. W. *J. Phys. Chem.* **1987**, *91*, 1099.

Table XV. Kinetic Data for the Chlorine-Atom-Transfer Reactions from the Chloroalkanes to $(OC)_4ReBr^{\bullet-}$, $(OC)_4ReCl^{\bullet-}$, and $(OC)_5Cr^{\bullet-}$ and the Thermal Electron Attachment Rate Constants, k_{TEA}, of the Chloroalkanes

RCl	k_{TEA},[a] cm^3 $molecule^{-1}$ s^{-1}	k_{total}, cm^3 $molecule^{-1}$ s^{-1}		
		$(OC)_4ReBr^{\bullet-}$[b]	$(OC)_4ReCl^{\bullet-}$[c]	$(OC)_5Cr^{\bullet-}$[d]
CCl_4	3.9×10^{-7}	1.6×10^{-10}	1.7×10^{-10}	2.5×10^{-10}
CCl_3F	2.6×10^{-7}	3.9×10^{-11}	4.7×10^{-11}	1.1×10^{-10}
CCl_2FCClF_2	3.9×10^{-8}	4.1×10^{-11}	4.2×10^{-11}	1.7×10^{-10}
CCl_3CH_3	1.6×10^{-8}	3.1×10^{-12}	3.2×10^{-12}	8.0×10^{-12}
$CHCl_3$	4.4×10^{-9}	1.1×10^{-12}	1.3×10^{-12}	6.1×10^{-12}
CCl_2F_2	3.2×10^{-9}	5.5×10^{-13}	1.4×10^{-13}	5.2×10^{-12}
CH_2Cl_2	4.8×10^{-12}	$<10^{-13}$	$<10^{-13}$	$<10^{-13}$
CF_3Cl	1.8×10^{-13}	$<10^{-13}$	$<10^{-13}$	$<10^{-13}$
CH_3Cl	$<2 \times 10^{-15}$	$<10^{-13}$	$<10^{-13}$	$<10^{-13}$

[a] From Table XII. [b] From Table I. [c] From Table II. [d] From Table IX.

Table XVI. Lower Limits of the Bond Energies $D°(L(OC)_{x-1}M^{-}-X)$

$L(OC)_{x-1}M-X^-$	lower limit of bond energy, kcal mol^{-1}		
	X = Cl	X = Br	X = I
$(OC)_4ReBr^{-}$-X	79.2	70.6	57.2
$(OC)_4ReCl^{-}$-X	79.2	70.6	57.2
$(OC)_4MnBr^{-}$-X	70.3	70.6	55.0
$(OC)_4MnCl^{-}$-X	70.3	70.6	55.0
$(\eta^3\text{-}C_3H_5)Re(CO)_3^{-}$-X	82.8	70.6	57.2
$(\eta^3\text{-}C_3H_5)Mn(CO)_3^{-}$-X	70.3		57.2
$(OC)_5Cr^{-}$-X	79.2	70.6	57.2
$(OC)_4Fe^{-}$-X	70.3	70.6	55.0
$(OC)_3Ni^{-}$-X	79.2	70.9	55.0

$(OC)_3Ni^{\bullet-}$, $(OC)_5Cr^{\bullet-}$, and $(OC)_4ReBr^{\bullet-}$ and the small data sets of $(OC)_4Fe^{\bullet-}$ and $(OC)_4MnBr^{\bullet-}$. The data sets for $(OC)_4ReCl^{\bullet-}$ and $(OC)_4MnCl^{\bullet-}$ were omitted for clarity since they were quite similar to those of the corresponding bromide metal complex negative ions with the same haloalkanes. The alkyl halides include the chloroalkanes CCl_4, $CFCl_3$, CCl_2FCClF_2, CH_3CCl_3, and CF_2Cl_2 which yielded the products of Cl-atom transfer, and CH_3I and CF_3Br, which gave the products of I- and Br-atom transfer, respectively. The log–log plot was needed to incorporate the data since the k_{TEA}'s cover a range of $>10^2$ while the range of the k_{total} is $\approx 10^4$.

There are a number of features in Figure 1 that deserve comment. First, we note that the trends in the rate constants of these reactions are reasonably correlated by the k_{TEA} values for the various haloalkanes with some exceptions. As mentioned above, the relative value of k_{TEA} for CCl_2FCClF_2 appeared to be small on the basis of the rate constants measured for Cl-atom-transfer reactions to $(OC)_4ReBr^{\bullet-}$, $(OC)_4ReCl^{\bullet-}$, and $(OC)_kCr^{\bullet-}$ in Table XVI. This is clearly shown in Figure 1. The remaining rate constants for Cl-atom transfer to these three metal complex negative ions vs the k_{TEA}'s for CCl_4, $CFCl_3$, CH_3CCl_3, $CHCl_3$, and CF_2Cl_2 show a reasonably good correlation in Figure 1. The correlation lines in Figure 1 include all of the data points shown.

The points for the reactions of $(OC)_4ReBr^{\bullet-}$ (and the chloride) and $(OC)_5Cr^{\bullet-}$ with CH_3I fall close to the values predicted for $k_{TEA}(CH_3I)$ on the basis of the above correlated Cl-atom transfer reactions for these metal complex negative ions. However, the measured rate constants for the Br-atom-transfer reactions from CF_3Br to these metal complex negative ions were considerably larger than were predicted by the reported value for $k_{TEA}(CF_3Br)$. This discrepancy is most clearly seen in comparing the k_{total} for the halogen-atom-transfer reactions of the above metal complex negative ions with CCl_3CH_3 and CF_3Br since $k_{TEA}(CCl_3CH_3) = k_{TEA}(CF_3Br) = 1.6 \times 10^{-8}$ cm^3 $molecule^{-1}$ s^{-1} (Table XII). The rate constants for Br-atom transfer to $(OC)_4ReX^{\bullet-}$ (X = Br or Cl) and $(OC)_5Cr^{\bullet-}$ from CF_3Br are $\approx$35 times larger than the rate constants for the analogous Cl-atom-transfer reactions with CCl_3CH_3. This problem carries over to the reactions of $(OC)_4Fe^{\bullet-}$ and $(OC)_4MnBr^{\bullet-}$ (and $(OC)_{3,4}MnCl^{\bullet-}$, not shown in Figure 1) where slow halogen-atom-transfer reactions were observed with CCl_4 ($k_{TEA} = 3.9 \times 10^7$ cm^3 $molecule^{-1}$ s^{-1}) and CF_3Br, but *no* reaction ($k_{total} < 10^{-13}$ cm^3 $molecule^{-1}$ s^{-1}) was observed with CCl_3F ($k_{TEA} = 2.6 \times 10^{-7}$ cm^3 $molecule^{-1}$ s^{-1}) or other chloroalkanes.

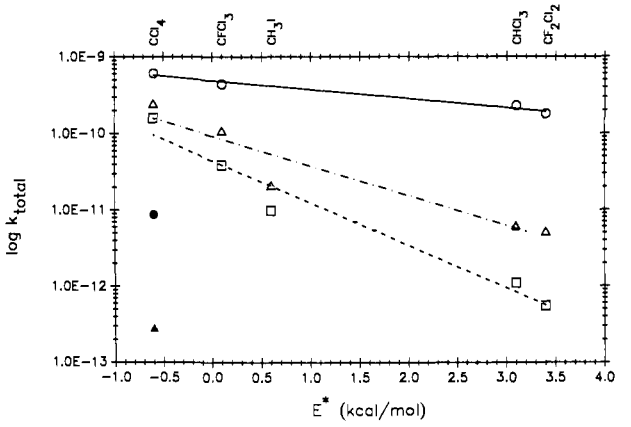

Figure 2. Plot of log k_{total} for the reactions of $(OC)_3Ni^{\bullet-}$ (○), $(OC)_5Cr^{\bullet-}$ (△), $(OC)_4ReBr^{\bullet-}$ (□), $(OC)_4Fe^{\bullet-}$ (●), and $(OC)_4MnBr^{\bullet-}$ (▲) with the RX molecules listed along the top axis vs the activation energies (E^*) for thermal electron attachment to these haloalkanes. Correlation lines (solid for $(OC)_3Ni^{\bullet-}$, –·– for $(OC)_5Cr^{\bullet-}$, and – – – for $(OC)_4ReBr^{\bullet-}$) include all of the data points.

The above observations and considerations lead us to the conclusion that the reported $k_{TEA}(CF_3Br)$ is in error and that it should be $>k_{TEA}(CCl_3F)$ and close to that of $k_{TEA}(CCl_4)$. This change would mean that the slopes for the $(OC)_4Fe^{\bullet-}$, $(OC)_4MnBr^{\bullet-}$, and $(OC)_4MnCl^{\bullet-}$ data would be very steep.

Wentworth et al.[35] measured the activation energies (E^*) for attachment of thermal energy electrons to a series of alkyl halides over the temperature range 303–493 K. These authors noted that "the relationship between the energy of activation (E^*) and the change in the internal energy (ΔE) for the dissociative electron attachment reaction is uniquely linear with approximately unit slope". A plot of the present data for halogen-atom transfer (298 K) vs E^* for the haloalkanes common to both studies reacting with $(OC)_3Ni^{\bullet-}$, $(OC)_5Cr^{\bullet-}$, $(OC)_4ReBr^{\bullet-}$, $(OC)_4Fe^{\bullet-}$, and $(OC)_4MnBr^{\bullet-}$ is given in Figure 2; the data for $(OC)_4ReCl^{\bullet-}$ and $(OC)_4MnCl^{\bullet-}$ very similar to those of the corresponding bromide complexes are omitted for clarity. Similar correlations of k_{total}'s for the halogen-atom-transfer reactions of these 17-electron transition-metal complexes are found in Figures 1 and 2. Unfortunately, the E^*'s for CF_3Br[36] and CH_3CCl_3 have not been determined. There is no correlation between the E^*'s and the thermodynamic EA_T's of CCl_4, $CHCl_3$, $CFCl_3$, CF_2Cl_2, CF_3Cl, CH_3Br, and CH_3I.

The correlations in Figures 1 and 2 of the present kinetic data for halogen-atom transfer between the 17-electron transition-metal complex negative ions and the haloalkanes with the process of

(35) Wentworth, W. E.; George, R.; Keith, H. *J. Chem. Phys.* **1969**, *51*, 1791. The haloalkanes and their E^*'s (in kcal mol^{-1}) used in the present study were CCl_4 (0.6 ± 0.1), $CFCl_3$ (0.1 ± 0.1), CH_3I (0.6 ± 0.1), $CHCl_3$ (3.1 ± 0.2), and CF_2Cl_2 (3.4 ± 0.1).

(36) The E^*'s[35] reported for CH_3Cl (12.5 ± 0.4 kcal) and CH_3Br (5.7 ± 0.4 kcal) differ by $\approx$7 kcal. If this same difference applies to the pair CF_3Cl (7.5 ± 0.4 kcal) and CF_3Br, then $E^*(CF_3Br) \approx 0$ kcal mol^{-1} would be expected, which would support our contention that $k_{TEA}(CF_3Br) > 1.6 \times 10^{-8}$ cm^3 $molecule^{-1}$ s^{-1}.

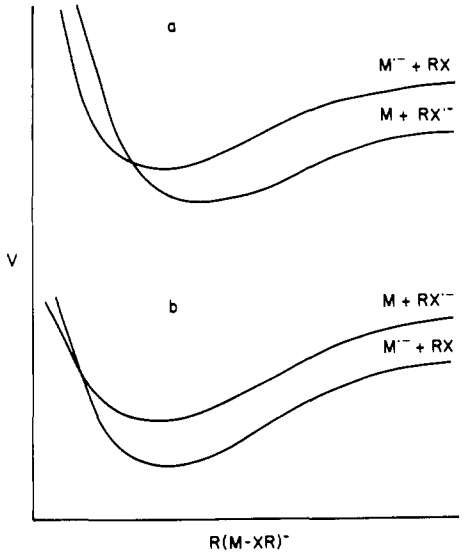

Figure 3. Schematic representations of curve crossings for (a) an efficient, exothermic and (b) an inefficient, endothermic electron tranfer between the metal complex $M^{\bullet-}$ and the RX molecules. The chemistry of the dissociative transfer of X^- from $RX^{\bullet-}$ to M is linked to the curve crossing on a different coordinate. The $MX^- + {}^\bullet R$ channel is believed to be the most exothermic exit channel for all of these reactions.

attaching thermal energy electrons to the haloalkanes (k_{TEA} and E^*) mean that electron transfer controls k_{total} in these reactions. The electron-jump or "harpoon" mechanism introduced to explain the large cross sections for alkali metal–halogen reactions[37] and its extensions to include the related halogen-atom transfers from alkyl halides[31] serve as a starting point in our considerations. Since both the k_{TEA}'s and E^*'s for thermal electron attachment to the haloalkanes involve the *vertical* EA's (EA_V) of the haloalkanes,[38] we can now understand why the attempt to correlate the present rate constants for halogen-atom transfer with the thermodynamic EA_T's of the haloalkanes (Table XIV) failed.

The general mechanism considered to be operating in these reactions is that given in eq 17. Step a is the formation of the ion/haloalkane collision complex **4** generated with a rate constant k_{ADO} or k_{LAN}[17] with a well depth of 10–20 kcal mol^{-1} [39] due to the attractive ion–dipole and ion–induced dipole forces. Electron transfer within this complex (step b) would yield complex **5** containing the 16-electron metal structure $L(OC)_{x-1}M$ and the reduced haloalkane $RX^{\bullet-}$, the latter likely to be formed in either a repulsive state or on the repulsive wall of a weakly bound state.[33] Since the lifetime of $RX^{\bullet-}$ in **5** is expected to be very short (possibly one vibrational period[33]), step c converting complex **5** into complex **6** would likely have no barrier. Separation of complex 6 (step d) would then yield the products of the halogen-atom-transfer reaction.

As in the reactions of the alkali-metal atoms with the halogens and haloalkanes, the present halogen-atom-transfer reactions are formulated as crossing of diabatic potential energy surfaces. This curve crossing occurs in the electron-transfer step where the attractive potential surface of $L(OC)_{x-1}M^{\bullet-} + RX \rightarrow$ **4** switches to that of the surface for $L(OC)_{x-1}M + RX^{\bullet-} \rightarrow$ **5**. The components of the collision complex **5** cannot separate due to the short lifetimes of $RX^{\bullet-}$ and, in most instances, separation would be endothermic. The short-range crossing points for these surfaces probably vary considerably and are dependent on both the metal complex and on the nature of R in RX.

In the reaction of $(OC)_3Ni^{\bullet-}$ with CCl_4, which occurred at nearly the collision limit, electron transfer will be exothermic by $\approx$1 eV since $EA_T(CCl_4) = 2.0$ eV (Table XII) and $EA_T(Ni(CO)_3) = 1.077 \pm 0.013$ eV.[40] The exothermic electron transfer is likely to produce vibrationally excited $CCl_4^{\bullet-}$, which rapidly dissociates to yield the complex $[(OC)_3NiCl^-/{}^\bullet CCl_3]^*$; the lifetime of the complex $[(OC)_3Ni/Cl_4^{\bullet-}]^*$ could be as short as one vibrational period.[33] The high efficiency of this reaction ($k_{total}/k_{ADO} = 0.67$) suggests that the curve crossing occurs close to the energy minimum collision complex $[(OC)_3Ni^{\bullet-}/CCl_4]^*$ with little or no barrier; see Figure 3a. That the electron transfer occurs within the collision complex appears to be required since we do not observe the formation of Cl^- which would be expected if electron transfer occurred at a large separation distance of $(OC)_3Ni^{\bullet-}$ and CCl_4.

The corresponding reaction of $(OC)_4Fe^{\bullet-}$ with CCl_4 proceeded with a much lower reaction efficiency (0.011). In this reaction, electron transfer is endothermic ($EA_T(Fe(CO)_4) = 2.4 \pm 0.3$ eV).[41] Since it appears unlikely that adduct metal complex negative ions of the structure $L(OC)_{x-1}MXR^{\bullet-}$ are energy minima in the gas phase, the observed slow reaction between $(OC)_4Fe^{\bullet-}$ and CCl_4 is consistent with curve crossing occurring well above the minimum energy of the ion–molecule collision complex $[(OC)_4Fe^{\bullet-}/CCl_4]^*$; see Figure 3b. This would effectively introduce a barrier to the electron-transfer step and lower the efficiency of this step, which would allow for dissociation of the collision complex to starting ion and neutral leading to the small observed rate constant.

The EA_T's of the other seven neutral metal complexes used in the study are unknown. However, the present studies involve the EA_V's[37] of the neutral metal complexes. On the basis of the rate constants for their reactions with CCl_4, we suggest that the EA_V's of $Re(CO)_4X$ (X = Cl or Br), $M(\eta^3\text{-}C_3H_5)(CO)_3$ (M = Re or Mn), and $Cr(CO)_5$ are between $EA_V(Fe(CO)_4)$ and $EA_V(Ni(CO)_3)$ (probably closer to $EA_V(Fe(CO)_4)$), while the EA_V's of $Mn(CO)_{3,4}X$ (X = Cl or Br) $\geq EA_V(Fe(CO)_4)$. These suggested EA_V's assume that the curve crossing for electron transfer in the respective collision complexes of these metal complex negative ions with CCl_4 are mainly dependent on the EA_V's of the metal complexes.

Summary

The rate constants for halogen-atom (Cl, Br, and I) transfer reactions between 11 17-electron transition-metal complex negative ions and a series of haloalkanes have been measured in a flowing afterglow apparatus at 298 K. Correlations of the data sets from $(OC)_3Ni^{\bullet-}$, $(OC)_5Cr^{\bullet-}$, and $(OC)_4ReX^{\bullet-}$ (X = Cl or Br) were found with the rate constants (k_{TEA}) and activation energies (E^*) for thermal electron attachment to the haloalkanes but not with several thermodynamic parameters of the haloalkanes. These findings show that the mechanism of these reactions is electron transfer within the ion/molecule collision complex $[L(OC)_{x-1}M^{\bullet-}/RX]$ yielding $[L(OC)_{x-1}M/RX^{\bullet-}]$ followed by X^- transfer from $RX^{\bullet-}$ to the 16-electron metal complex $L(OC)_{x-1}M$ within the collision complex giving the products $L(OC)_{x-1}MX^{\bullet-}$ and $R^\bullet$.

Although the electron-transfer mechanism does not allow for the bracketing of $D°(L(OC)_{x-1}M^-X)$, it does allow for the assignment of lower limits to several M^-X bond dissociation energies. These are shown in Table XVI.

Acknowledgment. Support of this research by the National Science Foundation is gratefully acknowledged. We also thank Professor Donald Setser for advice and discussions.

Registry No. $(OC)_4ReBr^{\bullet-}$, 121175-62 $(OC)_4ReCl^{\bullet-}$, 121175-63-1; $(OC)_4MnBr^{\bullet-}$, 121175-64-2; $(OC)_3MnBr$ 121175-65-3; $(OC)_4MnCl^{\bullet-}$, 121175-66-4; $(OC)_3MnCl^{\bullet-}$, 121175 7-5; $(\eta^3\text{-}C_3H_5)Re(CO)_3^{\bullet-}$,

(37) Magee, J. L. *J. Chem. Phys.* **1940**, *8*, 687.

(38) Gislason et al. ((a) Goldfield, E. M.; Gislason, E. A.; Subelli, N. H. *J. Chem. Phys.* **1985**, *82*, 3179. (b) Goldfield, E. M.; Kosmas, A. M.; Gislason, E. A. *J. Chem. Phys.* **1985**, *82*, 3191) provide an explanation for why the "effective reactive" electron affinity need not be the vertical electron affinity in harpooning-type reactions.

(39) For example, Dougherty et al. (Dougherty, R. C.; Dalton, J.; Roberts, J. D. *Org. Mass. Spectrom.* **1974**, *8*, 77) reported the heats of association (ΔH in kcal mol^{-1}) of Cl^- with the chloromethanes: $CH_3Cl_2^-$, -8.6 ± 0.2; $CH_2Cl_3^-$, -15.5 ± 0.3; $CHCl_4^-$, -19.1 ± 0.7; CCl_5^-, -14.2 ± 0.7. The complexation energy of Cl^- with CH_3Cl has been calculated to be -10.3 kcal mol^{-1}; Chandrasekhar, J.; Smith, S. F.; Jorgensen, W. L. *J. Am. Chem. Soc.* **1985**, *107*, 154.

(40) Stevens, A. E.; Feigerle, C. S.; Lineberger, W. C. *J. Am. Chem. Soc.* **1982**, *104*, 5026.

(41) Engelking, P. C.; Lineberger, W. C. *J. Am. Chem. Soc.* **1979**, *101*, 5569.

121175-68-6; $(\eta^3\text{-}C_3H_5)Mn(CO)_3^{\bullet-}$, 121175-69-7; $(OC)_5Cr^{\bullet-}$, 39586-86-2; $(OC)_4Fe^{\bullet-}$, 51222-96-9; $(OC)_3Ni^{\bullet-}$, 51222-94-7; CCl_4, 56-23-5; $CHCl_3$, 67-66-3; CH_2Cl_2, 75-09-2; CH_3Cl, 74-87-3; CCl_3CH_3, 71-55-6; CCl_2FCClF_2, 76-13-1; CCl_3F, 75-69-4; CCl_2F_2, 75-71-8; $CClF_3$, 75-72-9; CH_3Br, 74-83-9; CF_3Br, 75-63-8; CCl_3Br, 75-62-7; CH_3I, 74-88-4; CF_3I, 2314-97-8; $(OC)_4ReBrCl^-$, 121175-70-0; $(OC)_4ReBr_2^-$, 44965-51-7; $(OC)_4ReBrI^-$, 44965-52-8; $(OC)_4ReCl_2^-$, 78295-38-2; $(OC)_4ReClI^-$, 121175-71-1; $(OC)_4MnBrCl^-$, 44965-45-9; $(OC)_4MnBr_2^-$, 51153-35-6; $(OC)_4MnBrI^-$, 37176-06-0; $(OC)_3MnBrCl^-$, 121175-72-2; $(OC)_3MnBr_2^-$, 121175-73-3; $(OC)_3MnBrI^-$, 121175-74-4; $(OC)_4MnCl_2^-$, 52901-71-0; $(OC)_4MnClI^-$, 121175-75-5; $(OC)_3MnCl_2^-$, 121175-76-6; $(OC)_3MnClI^-$, 121175-77-7; $(\eta^3\text{-}C_3H_5)Re(CO)_3Cl^-$, 121175-78-8; $(\eta^3\text{-}C_3H_5)Re(CO)_3I^-$, 121175-79-9; $(\eta^3\text{-}C_3H_5)Re(CO)_2I^-$, 121175-80-2; $(OC)_5CrCl^-$, 14911-56-9; $(OC)_4CrCl^-$, 121175-81-3; $(OC)_5CrBr^-$, 14911-72-9; $(OC)_5CrI^-$, 14911-71-8; $(OC)_4FeCl^-$, 88083-34-5; $(OC)_4FeBr^-$, 88083-31-2; $(OC)_2Fe(Br)(CF_3)^{\bullet-}$, 88083-33-4; $(OC)_4FeI^-$, 44864-27-9; $(OC)_2Fe(I)(CF_3)^{\bullet-}$, 88105-33-3; $(OC)_3NiCl^-$, 44635-04-3; $(OC)_2NiCl^-$, 121175-82-4; $(OC)_3NiBr^-$, 44635-03-2; $(OC)_2NiBr^-$, 121175-83-5; $(OC)_3NiI^-$, 36830-71-4; $(OC)_2NiI^-$, 121175-84-6; $(OC)_3ReBrCl^-$, 121175-85-7; $(OC)_3ReBr_2^-$, 121175-86-8; $(OC)_3ReCl_2^-$, 121175-87-9.

Reversible Interaction of Dioxygen with $MnPEt_3Br_2$

H. D. Burkett and S. D. Worley*

Contribution from the Department of Chemistry, Auburn University, Auburn, Alabama 36849.
Received December 19, 1988

Abstract: The reversible interaction of dioxygen with a solid-state $MnPEt_3Br_2$ film at −30 °C has been observed. Infrared spectroscopic evidence and isotopic labeling studies have shown that the reversible dioxygen species formed is of the side-on peroxo variety. This work represents the first unambiguous spectroscopic observation of the reversible interaction of dioxygen with solid-state $MnPR_3X_2$ complexes.

Several years ago McAuliffe and co-workers reported the synthesis and properties of a series of manganese(II) complexes of composition $MnLX_2$ (L = tertiary phosphine, X = anion), which they suggested interacted reversibly with dioxygen.[1] Subsequent reports by Green et al.,[2] and from these laboratories,[3,4] showed that a reversible interaction of the complexes with dioxygen was indeed controversial. While the Green laboratory could find no evidence of such a reversible interaction for THF solutions of the alleged complexes,[2] we reported that the solid-state complex $MnPEt_3Br_2$ did exhibit a ligand infrared band at 1030 cm^{-1}, which cycled in intensity upon dioxygen exposure/removal cycles at ambient temperature.[4] However, we observed that the possible reversible dioxygen interaction was accompanied by a competitive irreversible decomposition process to the corresponding manganese phosphine oxide complex. We were not able to detect a dioxygen infrared band for the phosphine complex, which cycled in intensity upon exposure and removal of the dioxygen, although a band at 1130 cm^{-1} suggestive of a superoxo species was observed. Wickens and Abrams later reported the preparation and analyses of complexes having formulae $MnX_2(PMe_2Ph)$ (X = Cl, Br, I, or NCS), but although they observed dramatic color changes upon exposure to dioxygen, they could not detect reversibility within the constraints of their experiment.[5] The current work has spectroscopically identified unambiguously for the first time a reversible interaction of dioxygen with a $MnLX_2$ complex.

Experimental Section

We have found that during preparation of active solid-state films of $MnLX_2$ complexes water and air must be completely excluded from the reaction vessel; sample manipulation in an inert atmosphere in a drybox is not sufficient. In this work a new infrared cell reactor was designed that solved the problem. The cell (Figure 1), which was constructed from a 64-mm Pyrex tube, contained two external KRS-5 infrared windows along one axis held in place by Torr Seal vacuum epoxy and, on the axis perpendicular to that containing the IR windows, a quartz sublimation furnace and a port through which a volatile sample could be introduced. A third infrared window (KBr) was attached to a manipulator, which allowed rotation of the window into the infrared beam or facing the sublimator or volatile-sample-introduction port. The KBr window could be heated resistively by nichrome wire or cooled by chilled gas, e.g., liquid-nitrogen boiloff; its temperature was monitored by a chromel–alumel thermocouple. The cell could be evacuated to ca. 10^{-6} Torr by a cryopump/ion pump system.

The complex films used in this study were prepared as follows. Anhydrous $MnBr_2$ was placed in the quartz sublimator portion of the cell and was degassed under vacuum at 380 °C for 48 h; the KBr window was baked at 250 °C during the same time. Then $MnBr_2$ was sublimed onto the KBr window as a thin film by heating the salt at 550 °C for about 50 min at a pressure of 2×10^{-6} Torr. The film was then exposed to triethylphosphine at its vapor pressure for 10 min at room temperature to produce the complex $MnPEt_3Br_2$ as a film on the KBr window. Although it is not possible to directly verify that the film has the stated stoichiometry due to its sensitivity to dioxygen and moisture, previous work here based upon dramatic changes in the infrared spectrum of the film relative to that of free triethylphosphine and the formation of the phosphine oxide complex (analyzed as $MnOPEt_3Br_2$) upon decomposition of the complex after extensive exposure to dioxygen at ambient temperature provided compelling indirect evidence that the stoichiometry of the complex film is $MnPEt_3Br_2$.[4] Following evacuation of the excess and uncoordinated PEt_3 at room temperature for 165 min, the sample was cooled to −30 °C under evacuation, and an infrared spectrum was recorded (IBM 32/AT FTIR). Then the sample film was ready to be exposed to dioxygen.

The anhydrous $MnBr_2$ (Aldrich Chemical Co.) employed in this work had a stated purity of 99% and was used without further purification (except for the sublimation process in the cell reactor). Triethylphosphine (Strem Chemical Co.) was distilled onto 3A molecular sieves and subjected to freeze/thaw evacuation cycles before use. $^{16}O_2$ obtained from Matheson (99.99%) was further purified before use by passage through a molecular sieve trap at 195 K. $^{18}O_2$ (99.5%) was obtained from ICN Stable Isotopes and used without further purification.

Results and Discussion

A $MnPEt_3Br_2$ film prepared as described above was exposed to 56 Torr of $^{16}O_2$ at −30 °C (causing a dark red color), and the FTIR was monitored periodically over several hours. Although some of the ligand bands were affected by the interaction of the complex with dioxygen, the most notable change in the spectrum

(1) For example, see: McAuliffe, C. A.; Al-Khateeb, H.; Jones, M. H.; Levason, W.; Minten, K.; McCullough, F. P. *J. Chem. Soc., Chem. Commun.* **1979**, 736-738. McAuliffe, C. A. *J. Organomet. Chem.* **1982**, *228*, 255-264.
(2) Brown, R. M.; Bull, R. E.; Green, M. L. H.; Grebenik, P. D.; Martin-Polo, J. J.; Mingos, D. M. P. *J. Organomet. Chem.* **1980**, *201*, 437-446.
(3) Burkett, H. D.; Newberry, V. F.; Hill, W. E.; Worley, S. D. *J. Am. Chem. Soc.* **1983**, *105*, 4097-4099.
(4) Newberry, V. F.; Burkett, H. D.; Worley, S. D.; Hill, W. E. *Inorg. Chem.* **1984**, *23*, 3911-3917.
(5) Wickens, D. A.; Abrams, G. *J. Chem. Soc., Dalton Trans.* **1985**, 2203-2204.

0002-7863/89/1511-5992$01.50/0